UNSUPERVISED CLASSIFICATION OF HYPERSPECTRAL IMAGES BY USING LINEAR UNMIXING ALGORITHM

Bin Luo and Jocelyn Chanussot

GIPSA-Lab, 961 rue de la Houille Blanche, 38402 Grenoble, France.
({Bin.luo, jocelyn.chanussot}@gipsa-lab.inpg.fr)

ABSTRACT

In this paper, we present an unsupervised classification algorithm for hyperspectral images. For reducing the dimension of hyperspectral data, we use a linear unmixing algorithm to extract the endmembers and their abundance maps. Compared to the components obtained by traditional PCA-based method, the abundance maps have physical meanings (such as the abundance of vegetation). For determining the number of endmembers contained in an image, we propose an eigenvalue based approach. The validation of this approach on synthetic data shows that this approach provides a robust estimation of the actual number of endmembers. Using the estimated abundance maps of the endmemebers, we perform a preliminary segmentation and use the mean values of the segmented regions as feature for the classification. We then perform Kmeans classifications on the segmented abundance maps with the number of clusters determined by the Krzanowski and Lai's method.

1. INTRODUCTION

The classification of hyperspectral remote sensing images is a challenging task, since the data dimension is considerable for traditional classification algorithms, typically several hundreds of spectral bands are acquired for each image. Moreover, due to physical constraints, hyperspectral data are corrupted by a higher amount of noise when compared to panchromatic or multispectral data. Therefore, for classification, it is desirable to reduce the dimension of the data, both for accelerating the classification algorithm and for reducing the influence of the noise. In [1], PCA-based methods are proposed to reduce the dimension of hyperspectral data. The components with significant variances are used as features for the classification. However, PCA-based methods present two main drawbacks. Firstly, the number of components used for classification is not easy to determine since the variance of noise can be similar to the variance of useful components. Moreover, the components obtained by these methods do not necessarily have physical meanings. As mentioned precedently, the components obtained by PCA could be noise or artifacts, if their variance is important. An alternative for reducing the dimension of hyperspectral data is to use the abundance maps of the chemical species present in the image obtained by unmixing algorithms. We assume that the spectrum of each pixel is the linear mixture of the spectra of different chemical species. Since the abundances of these species are positive, it is possible to determine the number of the species based on the difference of the eigenvalues of the correlation and covariance matrix. With the help of this number, by using linear unmixing algorithm, such as the VCA [2], we can obtain the spectra of the chemical species (referred to as endmembers) in the image, as well as the abundance maps, which can be then used for the classification.

In this paper, we present a totally unsurpervised classification chain for hyperspectal images. We propose at first an approach for determining the number of endmembers. With the help of the estimated number, we use VCA to unmix the spectrum of each pixel in the image in order to obtain the abundance maps of the endmembers. Afterwards, Kmeans is used in order to cluster the abundance maps for the classification of the hyperspectral image. Since the classification chain is totally unsupervised, the number of the clusters is automatically determined by Krzanowski and Lai's method [3].

2. LINEAR UNMIXING OF HYPERSPECTRAL DATA

2.1. Mathematical model

We note $\mathbf{X}$ the matrix representing the hyperspectral image cube, where $\mathbf{X} = \{\mathbf{x}_1, \mathbf{x}_2, \ldots, \mathbf{x}_{N_a}\}$ and $\mathbf{x}_k = \{x_{1,k}, x_{2,k}, \ldots, x_{N_s,k}\}^T$, $x_{l,k}$ is the value of the kth pixel at the lth band. We assume that the spectrum of each pixel is a linear mixture of the spectra of N_c endmembers, leading to the following model:

$$\mathbf{X} = \mathbf{MS} + \mathbf{n} \tag{1}$$

where $\mathbf{M} = \{\mathbf{m}_1, \mathbf{m}_2, \ldots, \mathbf{m}_{N_c}\}$ is the mixing matrix where $\mathbf{m}_n$ denotes the spectral signature of the nth endmember. $\mathbf{S} = \{\mathbf{s}_1, \mathbf{s}_2, \ldots, \mathbf{s}_{N_c}\}^T$ is the abundance matrix where $\mathbf{s}_n = \{s_{n,1}, s_{n,2}, \ldots, s_{n,N_a}\}$ ($s_{n,k} \in [0,1]$ is the abundance of the nth endmember at the kth pixel). $\mathbf{n}$ stands for the additive noise of the image. For separating $\mathbf{M}$ and $\mathbf{S}$ from

This work is funded by French ANR project VAHINE.

X without any *a priori* information, we have to estimate the number N_c of endmembers. In a second step, we can perform a linear unmixing in order to obtain **M** and **S**.

2.2. Estimation of the number of endmembers

In [4], it is proposed to threshold the eigenvalues of the covariance and correlation matrix for estimating the number of endmembers. We note K the sample covariance matrix of **X** and R its correlation matrix. Suppose that λ_i and $\hat{\lambda}_i$ are respectively the ith eigenvalues of K and R with $i \geq 0$, $\lambda_i > \lambda_{i+1}$ and $\hat{\lambda}_i > \hat{\lambda}_{i+1}$. Theoretically, if there are N_c endmembers present in **X**, the eigenvalues $\hat{\lambda}_i, (i > N_c)$ and $\lambda_i, (i > N_c)$ correspond to the noise variance, we have therefore:

$$\begin{cases} \hat{\lambda}_i - \lambda_i > 0, & i \leq N_c \\ \hat{\lambda}_i - \lambda_i = 0, & i > N_c \end{cases} \tag{2}$$

Noting $z_i = \hat{\lambda}_i - \lambda_i$, a Neyman-Person test can be used to threshold the z_i value in order to estimate the number of endmembers [4]. However, this method has two main drawbacks. Firstly, we have to fix a false alarm value in order to determine the threshold for z_i, which affects the estimated number. Secondly, if the artifacts (or noise) are not zero mean, this method can not give the exact number of endmembers. In this section, we propose a likelihood function based on Equation (2) for determining the number of endmembers. In [5], it is shown that the distribution of z_i can be modeled by

$$\begin{array}{ll} z_i \sim \aleph(\mu_i, \sigma_i^2), & i \leq N_c \\ z_i \sim \aleph(0, \sigma_i^2), & i > N_c \end{array} \tag{3}$$

where μ_i is unknown and σ_i can be given by $\sigma_i^2 \approx \frac{2}{N}(\hat{\lambda}_i^2 + \lambda_i^2)$, if the number of samples are sufficiently large (which is usually the case for hyperspectral images) [4][5]. According to Equation (3), we define a likelihood function $H(i) = \Pi_{l=i}^{N_s} \frac{1}{\sigma_l} \exp(-\frac{z_l^2}{2\sigma_l^2})$ and

$$\tilde{H}(i) = \log H(i) = -\sum_{l=i}^{N_s} \frac{z_l^2}{2\sigma_l^2} - \sum_{l=i}^{N_s} \log \sigma_l \tag{4}$$

$\tilde{H}(i)$ will have a global *maximum* when $i = N_c + 1$.

In practice, we found by experiments that, if the hyperspectral images have N_{art} bands corrupted by artifacts (with non zero means), the global *maximum* of $\tilde{H}(i)$ will be at $i = N_c + N_{art} + 1$. However, at $i = N_c + 1$, $\tilde{H}(i)$ will have a local *maximum*. Therefore, in practice, we define the number of endmembers as:

$$\hat{N}_c = \min_i \{\tilde{H}(i-1) \leq \tilde{H}(i) / \tilde{H}(i+1) \leq \tilde{H}(i)\} - 1 \tag{5}$$

In order to validate our method for estimating the number of endmembers, we have simulated hyperspectral data by using the reflective spectra of three endmembers, *i.e.* $N_c = 3$.

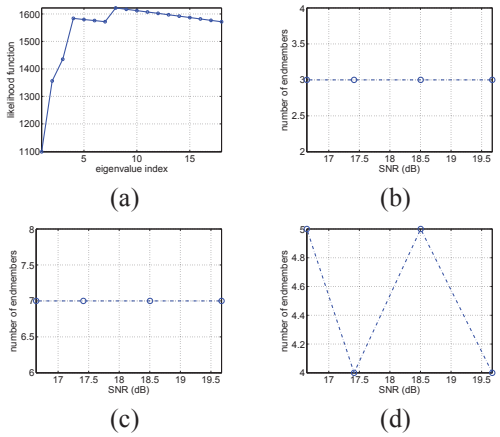

Fig. 1. (a) Likelihood function $\tilde{H}(i)$ when $SNR = 17.4dB$; (b) $\hat{N}_c$ as the function of SNR obtained by Equation (5); (c) values of $\arg\max_i\{\tilde{H}(i)\} - 1$; (d) number of endmembers estimated by the method of [4].

The abundances of these endmembers are positive and distributed by Gaussian distributions. The sum of the abundances at each pixel is equal to one, *i.e.* $\forall k, \sum_{n=1}^{N_c} s_{n,k} = 1$. We add Gaussian additive noise with zero mean. In order to simulate the artifacts, we add Gaussian noise with non zero mean at four bands ($N_{art} = 4$). In Figure 1(a), we have shown $\tilde{H}(i)$ when the $SNR = 17.4dB$. We can observe that there are two local *maxima*, one is at $i = 4$, which corresponds to $N_c + 1$, another is at $i = 8$, which corresponds to $N_c + N_{art} + 1$. We have tested our approach with 4 different noise levels. The number N_c estimated by Equation (5) is shown in Figure 1(b). It can be observed that $\hat{N}_c$ estimated is always equal to 3. Figure 1(c) shows the position $\arg\max_i\{\tilde{H}(i)\} - 1$ with different noise levels. It can be seen that the global maixmum always corresponds to $N_c + N_{art} = 7$. In Figure 1(d), we show the numbers of endmembers estimated by the method in [4] with different noise levels. We can see that this method gives the numbers between N_c and $N_c + N_{art}$.

2.3. Vertex Component Analysis (VCA)

In [2], the Vertex Component Analysis (VCA) is proposed as an effecient method for extracting the endmembers which are linearly mixed. The main idea is to extract the vertex of the simplex formed by **M** which contains all the data vectors in **X**. According to the sum-to-one condition, the sum of the abundances of all the endmembers for each pixel is equal to one, *i.e.* $\forall k, \sum_{n=1}^{N_c} s_{n,k} = 1$. Therefore the data vectors $\mathbf{x}_l$ are always inside a simplex of which the vertex are the spectra of the endmembers. VCA iteratively projects the data onto the direction orthogonal to the subspace spanned by the endmembers already determined. And the extreme of this projection is the new endmember signature. The algorithm stops the iteration when all the p endmembers are extracted, where p is

the number of endmembers which has to be fixed before performing VCA. In practice, we fix $p = \hat{N}_c$ determined by the approach presented in Section 2.2.

3. UNSURPERVISED CLASSIFICATION BASED ON THE ABUNDANCES OF THE ENDMEMBERS

3.1. Preliminary segmentation

As the hyperspectral data are usually very noisy, we perform a preliminary segmentation of each abundance map in order to regularize the classification results. The segmentation is based on the algorithm presented in [6]. The abundance map $\mathbf{s}_n$ is firstly represented by an inclusion tree of connected components of its level sets. For each pixel $s_{n,k}$ in the nth abundance map, there is a branch of the tree made by all the connected components containing this pixel. The bottom of this branch is the smallest component containing this pixel and the top is the whole image. With the help of this inclusion tree, for each pixel, we select the component containing it, of which the contrast (which is the absolute difference between to succesive components) is the most important, as the most significant components for this pixel. All such components form a partition of the image. Afterwards, we associate the mean value of the component to the pixel as the feature for classification. We note $\bar{s}_{n,k}$ the mean value of the most contrasted component at the kth pixel on the nth abundance map.

3.2. Kmeans clustering

We have chosen the Kmeans algorithm to cluster the abundance maps. For Kmeans clustering, we have to fix the number of clusters. It has to be noticed that the number of clusters and the number of endmembers are different. The endmembers are the chemical species present in an image, such as water, vegetation, etc. While the clusters have more semantic meanings. A cluster can correspond to the regions where one single endmember has high proportion. It can also correspond to the mixture of several endmembers. We use Krzanowski and Lai's method [3] for determining the number of clusters. Note $W(g)$ the sum of the distances of the data vectors to the nearest cluster center, *i.e.* $W(g) = \sum_{i=1}^{g} \sum_{k \in \Omega_i} d(\bar{s}_{.,k} - C_i)$ where $\bar{s}_{.,k} = \{\bar{s}_{1,k}, \ldots, \bar{s}_{N_c,k}\}$ is the abundance vector at pixel k. Ω_i is the ith cluster, and C_i is its centroid. g is the number of clusters.

Let $D(g) = (g-1)^{\frac{2}{N_c}} W(g-1) + g^{\frac{2}{N_c}} W(g)$. According to [3], the number of clusters $\hat{K}$ is defined as:

$$\hat{K} = \arg\max\{KL(g)\} = \arg\max\left\{\left|\frac{D(g)}{D(g+1)}\right|\right\}. \quad (6)$$

4. CLASSIFICATION RESULTS

In this section, we present the classification results obtained on a hyperspectral image taken by the instrument ROSIS (Reflective Optics System Imaging Spectrometer) over the University of Pavia, Italy (see Figure 2(a)). The image (with a spatial resolution of $1.3m$) contains 340×610 pixels and 103 spectral bands covering visible and near infrared light. By using Equation (5), the number of endmembers contained in this image is 2. The two abundance maps obtained by VCA are presented in Figures 2(b) and (c). We observe that, Figure 2(b) corresponds to the abundance of bare soil, while Figure 2(c) corresponds to the vegetation. We then segment these two abundance maps by using the method introduced in Section 3.1. In Figures 2(d) and (e), we have shown the segmented images of Figure 2(b) and (c). The value of a pixel in Figures 2(d) and (e) is the mean value of the segmented region containing this pixel. We then perform Kmeans clustering on the segmented abundance maps with a number of clusters ranging from 2 to 16. By calculating the KL index (see Equation (6)) on the results of the clusterings, the optimal number of clusters is 6. As discussed in Section 3.2, the number of culsters can be different with the number of endmembers. For example, regions of different abundances of vegetations can be classified differently, such as meadows and trees. Moreover, combinations of several endmembers with different abundances can be classified as different classes. In Figure 3(a), we show the unsupervised classification results obtained by Kmeans on the segmented abundance maps with 6 clusters.

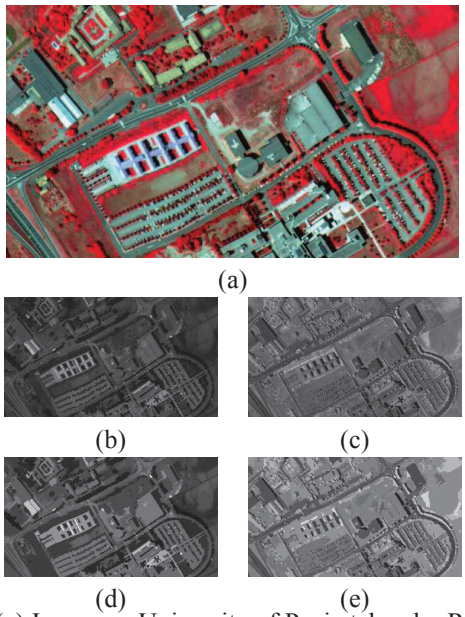

Fig. 2. (a) Image on University of Pavia taken by ROSIS instrument ©DLR (R-band 90, G-band 60, B-band 40); (b) and (c) abundance maps obtained by VCA; (d) and (e) segmented images obtained from (b) and (c), the value of each pixel corresponds to the mean value of the segmented region.

For comparison, the classification result obtained by Kmeans on the original dataset (without reducing the di-

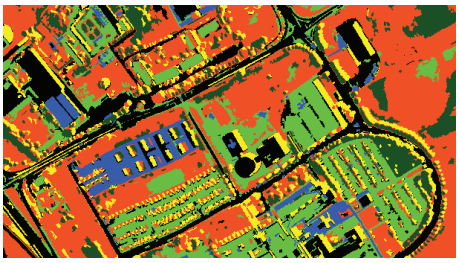

(a)

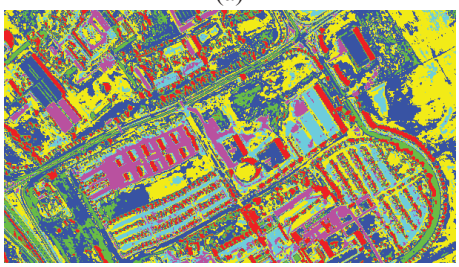

(b)

Fig. 3. (a) Unsupervised classification result of figure 2(a) obtained on the segmented abundance maps by Kmeans with 6 clusters. With the help of the ground truth , these clusters can be roughly identified as Meadows, Bare soil, Asphalt, Shadow, Tree, Metal roof. (b) Unsupervised classification result obtained on the original dataset with 6 clusters.

mension and preliminary segmentation) with 6 clusters is shown in Figure 3(b).

It is observed that the classification results in Figure 3(a) is accurate, especially the asphalt, the trees and the shadow are very well classified. However, since the roads and the roofs of some buildings are made by the same material (asphalt), they are classified in the same class. The classification of Figure 3(b) is not easy to interpret, since only the shadow can be identified. Other clusters obtained by Kmeans seem to be a mixture of several classes. For example, the yellow class is the mixture of meadow and asphalt (the round building in the middle of the image). It has to be noticed that even though the ground truth of manual classification of this image is available, it is still difficult to compare quantitatively the unsupervised classification results obtained by our approach with the manually classified ground truth, since the definitions of the classes are very different. The ground truth is used only for identify the classes obtained by unsupervised classification.

5. CONCLUSION

In this paper, we have presented a scheme for unsupervised classification of hyperspectral images. The first contribution of this work is the use if linear unmixing algorithm to extract endmembers and their abundance maps as features for the classification. When compared to tranditional dimension reduction approaches, such as PCA based methods, the abundance maps of endmembers have physical meanings (such as the distribution of vegetation, etc.). Moreover, for PCA-based methods, the number of the components used for classification is not easy to determine. While the number of endmembers present in an image can be estimated by using the difference of the eigenvalues of the covariance and correlation matrix of the hyperspectral data, which is the second contribution of this paper. In order to reduce the influence of noise and to regularize the classification results, a preliminary segmentation is then performed on the abundance maps. Finally, Kmeans clustering is performed on the segmented abundance maps with the number of clusters determined by KL index. The results obtained by this totally unsupervised classification algorithm shows that it can well classify the urbain objects made by different materials. However, since the classification is mainly based on the spectral information, further improvement can be done by taking into account the spatial information in order to separate the objects made by the same material but with different semantic meanings (such as roads and roofs of buildings).

Acknowlegdement

The authors would like to thank Pr. Paulo Gamba, University of Pavia, for providing the data and the ground truth of the classification.

6. REFERENCES

[1] M. Fauvel, J. Chanussot, and J. A. Benediktsson, "Kernel principal component analysis for the classification of hyperspectral remote-sensing data over urban areas," *EURASIP Journal on Advances in Signal Processing*, to appear.

[2] J. M. P. Nascimento and J. M. B. Dias, "Vertex component analysis: A fast algorithm to unmix hyperspectral data," *IEEE Trans. Geoscience and Remote Sensing*, vol. 43, no. 4, pp. 898 – 910, April 2005.

[3] W. J. Krzanowski and Y. T. Lai, "A criterion for determining the number of groups in a data set using sum of squares clustering," *Biometrics*, vol. 44, pp. 23–34, 1988.

[4] C. I. Chang and Q. Du, "Estimation of number of spectrally distinct signal sources in hyperspectral imagery," *IEEE Trans. Geoscience and Remote Sensing*, vol. 42, no. 3, pp. 608–619, March 2004.

[5] T.W. Anderson, *An introduction to multivariate statistical analysis*, Springer-Verlag, 2nd edition, 1984.

[6] B. Luo, J.-F. Aujol, and Y. Gousseau, "Local scale measure from the topographic map and application to remote sensing images," *SIAM Multiscale Modeling and Simulation*, to appear.